Dihydrogen Bonding

DOI: 10.1002/anie.201403690

Evidence of Dihydrogen Bonding of a Chiral Amine–Borane Complex in Solution by VCD Spectroscopy**

Christian Merten, Christopher J. Berger, Robert McDonald, and Yunjie Xu**

Abstract: *IR and vibrational circular dichroism (VCD) spectra of a chiral amine–borane in solution are investigated. By comparison of experimental and calculated spectra, unique VCD spectral signatures, which can be attributed to the formation of dihydrogen-bonded dimers in solution, are identified for the first time. These VCD features are highly sensitive to the specific dihydrogen-bonding topologies utilized by the chiral amine–borane subunits and thus provide direct structural information of these dihydrogen-bonded species in solution. Differences in the dihydrogen binding arrangements in solution and in solid state are also revealed.*

Ammonia–borane ($H_3N{\cdot}BH_3$) and related compounds have generated much excitement in the last ten years as potential hydrogen storage materials or dehydrogenation catalysts.[1] An extensive amount of work has been carried out to characterize these materials mainly in solid state but also in solution and in the gas phase using a wide variety of spectroscopic techniques. At the more fundamental level, amine–borane and many of its derivatives feature a special kind of hydrogen bond, that is, a dihydrogen bond (DHB) where the hydridic hydrogen is provided by the borane part of the molecule and the acceptor itself is also a hydrogen atom ($N{-}H^{\delta+}\cdots{}^{\delta-}H{-}B$).[2]

Since the first clear classification of this new type of hydrogen bonds by Crabtree, Siegbahn, and co-workers based on a comprehensive survey of the Cambridge Structure Database (CSD),[3] DHBs have attracted much attention from both theorists and experimentalists. Most experimental structural studies have been carried out using X-ray crystallography where in the N–H···H–B-type interactions, a DHB is characterized by an average H···H distance of 1.96 Å (ranging from 1.7–2.2 Å), an average N–H···H angle of 149° (ranging from 117–171°), and an average B–H···H angles of 120° (90–171°).[3] In the solid-state structures of ammonia–borane, the nitrogen and boron atoms are aligned and connected by two sets of DHBs in the tetragonal and three sets in the orthorhombic phase, respectively.[4] In their theoretical study, Cramer and Gladfelter revealed that the most stable gas phase geometry of $(H_3N{\cdot}BH_3)_2$ is a C_{2h}-symmetric head-to-tail structure with two sets of bifurcated DHBs.[5] The predicted H–H distance of 1.99 Å, and angles of 144.8° and 88.6° for N–H···HB and NH···H–B, respectively, were found to fall in the characteristic ranges mentioned above.

In solution, DHBs can be detected indirectly using IR and ^{1}H NMR spectroscopy by monitoring the change of characteristic vibrational frequencies or proton shifts.[2b] Although the first experimental data on DHBs were obtained using solution IR spectroscopy in the 1970s,[6] very few further IR studies of DHBs in solution have been reported, which is most likely due to the challenges in extracting any definite conclusion about DHB binding topologies from the broad-band spectral features, which may be contaminated by other H-bonding interactions in solution.[1,7]

Herein, we report the first study on a chiral amine–borane adduct, namely α-methylbenzyl amine–borane (MBA·BH_3, **1**; Scheme 1), in solution using vibrational circular dichroism (VCD) spectroscopy. VCD spectroscopy is highly sensitive to conformational changes and intra- and intermolecular interactions. It has been utilized not only for the determination of absolute configurations[8] but also for structural studies of a wide range of systems ranging from small molecules, such as metal complexes,[9] to (bio)polymers.[10] This sensitivity to intermolecular interactions has been manifested in studies on solvation of chiral molecules,[11] molecular self-aggregation,[12] and chirality induction to solvent molecules.[13] We now show unique VCD spectral signatures corresponding to the dihydrogen bonded dimers $(\mathbf{1})_2$ in solution by comparison of the experimental data with calculated spectra. The study shows that VCD spectroscopy is a powerful method to probe the binding topology of DHB systems directly in solution and its potential application to aid reaction mechanism studies involving DHBs in solution.

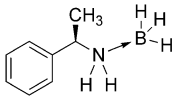

Scheme 1. Structure of the *R* enantiomer of the target molecule **1**.

The target molecule **1** is prepared by the simple reaction of enantiopure α-MBA with the borane adduct BH_3·DMS. Figure 1 shows the IR and VCD spectra that were recorded for 0.36 M solutions of both enantiomers of **1** in

[*] Dr. C. Merten
Lehrstuhl für Organische Chemie II, Ruhr-Universität Bochum
44801 Bochum (Germany)
E-mail: christian.merten@ruhr-uni-bochum.de
C. J. Berger, Dr. R. McDonald, Prof. Dr. Y. Xu
Department of Chemistry, University of Alberta
Edmonton, T6G2G2 (Canada)
E-mail: yunjie.xu@ualberta.ca

[**] This research was supported by the University of Alberta, the Natural Sciences and Engineering Research Council of Canada, and the Cluster of Excellence RESOLV (EXC 1069) of the Deutsche Forschungsgemeinschaft (DFG). We thank Prof. Eric Rivard for access to the synthesis equipment. C.M. acknowledges financial support by the Fonds der chemischen Industrie for a Liebig fellowship. Y.X. holds a Tier I (senior) Canada Research Chair in Chirality and Chirality Recognition. VCD = vibrational circular dichroism.

Supporting information for this article is available on the WWW under http://dx.doi.org/10.1002/anie.201403690.

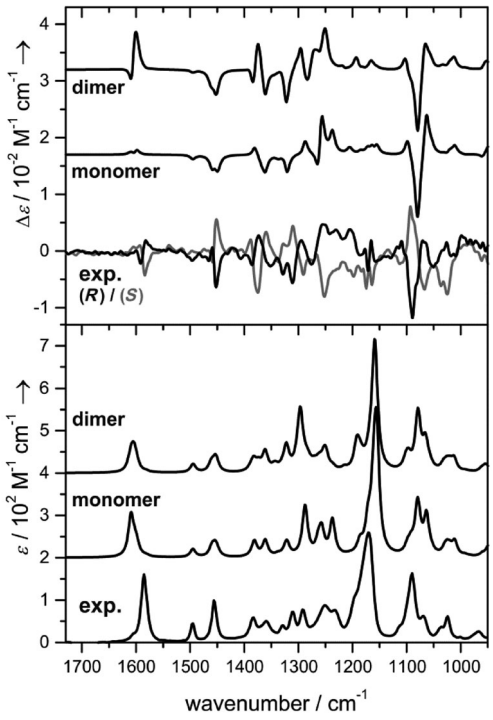

Figure 1. Experimental and calculated VCD (a) and IR spectra (b) of **1**. The experimental spectra are measured for a 0.36 M solution of **1** in [D_1]chloroform (path length 100 μm). The experimental IR spectra of both enantiomers are identical in this figure. The calculated spectra are offset for clarity.

[D_1]chloroform. The IR spectrum of **1** shows a few strong bands, including the clearly visible strong band of the NH_2 bending vibrations at about 1585 cm^{-1}, two sharp bands in the range of 1500–1450 cm^{-1} that are assigned to both the CH_3 deformation and aromatic C=C stretching vibration, and the BH_3 deformation modes at approximately 1170 cm^{-1}, to name a few. The spectral region from 1400–1200 cm^{-1} features many weak bands. We note that both the strong and the weak IR bands, on the other hand, feature strong and clearly resolved VCD bands. This advantage of the VCD spectral signatures enables us to identify each IR band that corresponds to a VCD band and vice versa. Especially noteworthy is the VCD pattern between 1200–1150 cm^{-1}, which corresponds to the B–H bending vibrations. It has been proposed that the vibrations of trifluoroborane (BF_3) become VCD active upon binding to a chiral amine.[14] As a similar outcome is also expected in the case of borane, the observation of this VCD pattern can be seen as an experimental verification of the hypothesis. Several attempts have also been made to measure the VCD signature of **1** in the BH stretching vibration (2500–2200 cm^{-1}). Consistent with the reported spectra of a chiral phosphane borane,[15] the bands in this region were found to be very broad, but the weak VCD signatures can still be recognized (Supporting Information, Figure S1).

To analyze experimental IR and VCD spectra, we first performed a potential energy surface scan of (*R*)-**1**, which revealed the existence of three local energy minima (B3LYP/6-31G(d); Supporting Information, Figure S3). They correspond to three possible conformations: *trans*-**1**, *gauche*(+)-**1**, and *gauche*(−)-**1**, which can be generated with respect to the torsion angle Ar-C*-N-B (Supporting Information, Figure S4). These three structures were further optimized at the B3LYP/6-311 + G(2d,p) level of theory while accounting for the effects of the solvent through the IEFPCM solvent model for chloroform.[16] According to the zero-point corrected relative energies obtained from these calculations, *trans*-**1** is favored over *gauche*(+)-**1** ($\Delta E = 0.8$ kcal mol^{-1}) and *gauche*(−)-**1** ($\Delta E = 2.8$ kcal mol^{-1}). These energy differences lead to Boltzmann populations of 79.3, 20.0, and 0.7 percent at room temperature, respectively. Similar results were obtained with dispersion corrections (B3LYP-GD3) and with the cc-pVTZ basis set (see the Supporting Information, Section S3).

The theoretical spectra of monomeric **1** shown in Figure 1 are based on the Boltzmann population weighted spectrum of the three conformers, that is, *trans*-**1**, *gauche*(+)-**1**, or *gauche*(−)-**1**. Furthermore, isotopic effect of boron with two isotopes with natural abundances of about 80 % ^{11}B and 20 % ^{10}B was also considered in the spectral simulation, although the isotope effect on the calculated monomer spectra was negligible (Supporting Information, Figure S5). The calculated IR spectrum of the monomer resembles most experimental bands reasonably well in position and relative intensity, but the comparison of the experimental and theoretical VCD spectra is much less satisfactory. Although the strong VCD pattern below 1150 cm^{-1} is captured by the calculation, the quality of the agreement decreases in the higher wavenumber region. The well-resolved −/+/− pattern (1400–1350 cm^{-1}) arising from CH and CH_3 bending vibrations, the −/+ VCD couplet around 1450 cm^{-1}, and the +/− VCD couplet of the NH_2 bending vibration at about 1585 cm^{-1} are all not well reproduced by the calculation. A detailed comparison and band assignments is provided in the Supporting Information, Figure S13.

For a relatively rigid and small molecule, a much better agreement between the experimental and theoretical spectra would be expected with the current state of experiments and theory. As the relative intensities of some IR bands were found to change slightly with concentration (for instance the two closely spaced bands around 1250 cm^{-1}; Supporting Information, Figure S2), we considered the formation of dimers in solution. Following previous theoretical studies,[5,17] we assumed **1** to form a head-to-tail dimer similar to the prototype dimer $(H_3N{\cdot}BH_3)_2$. As shown in the drawing in the Supporting Information, Figure S8, the head-to-tail structure can be accomplished with monomers in three different orientations relative to each other. Furthermore, each monomeric subunit can in general adopt either of the three conformations: trans-**1**, gauche(+)-**1**, or gauche(−)-**1**. When considering only the two major monomeric conformers, *trans*-**1** and *gauche*(+)-**1**, ten dimer configurations can be generated, which were optimized at the same level of theory employed for the monomer (see the Supporting Information, Table S3 for relative energies and populations). In the lowest-energy structure, the chiral substituents point towards the same side of the hydrogen-bonding plane (C_2 symmetric;

Supporting Information, Figure S8). The H–H distances (2.17 and 2.19 Å), and the N–H···HB (154.3 and 140.7°) and NH···H–B angles (92.8 and 91.9°) found for the C_2-symmetric dimer fall into the characteristic range for DHBs. In their theoretical study on the dimerization of $NH_3{\cdot}BH_3$, Cramer and Gladfelter also observed a shortening of the N–B bond (by 0.024 Å) and an elongation of the N–H bonds involved in DHBs (by 0.01 Å). We found similar but slightly smaller changes of the bond lengths (N–B shortened by 0.008 Å, and N–H elongated by 0.005 Å) for the C_2 dimer of **1**. These less-distinct bond length changes are reflected in the computed counterpoise-corrected complexation binding energy of 8.8 kcal mol^{-1} in the gas phase and the estimated interaction energy in solution of about 9.3 kcal mol^{-1}. For the related and well-studied $(H_3N{\cdot}BH_3)_2$, a binding energy of 15.1 kcal mol^{-1} was predicted.[5] The lower binding energy is most likely due to the higher steric demands of the phenylethyl substituents in $MBA{\cdot}BH_3$ compared to protons in $NH_3{\cdot}BH_3$.

In Figure 1, we compare the Boltzmann weighted IR and VCD spectra of dimeric **1** with the experimental spectrum. A remarkably better agreement is achieved between the experimental spectra and the spectra of the dimer than those of the monomer (see the Supporting Information, Figure S9 for further details). The w-shaped $-/+/-$ VCD band of the CH/CH_3 bending vibrations between 1400–1350 cm^{-1} as well as the $-/+$ VCD couplet of the amine bending vibrations (ca. 1585 cm^{-1}) are reproduced with the correct sign order and relative intensities. Only the VCD pattern at 1450 cm^{-1} is still missing its positive component. While both monomeric and dimeric species are likely to co-exist in solution (Supporting Information, Figure S2), the noticeable better agreement for the strong VCD bands clearly supports the dominant presence of dimeric **1** in solution. Similar results were obtained using the B3PW91 and B3LYP-GD3 functionals for the calculations.

A closer look at the particular IR and VCD spectra calculated for each of the ten dimer conformations further supports this conclusion (Supporting Information, Section S4). The examination reveals that the $-/+/-$ pattern between 1350–1400 cm^{-1} is characteristic for dimers with both monomer units in a *trans*-**1** conformation. In comparison with the experimental spectra, it can therefore be assumed that this combination must be clearly favored in solution. Furthermore, the pattern of the amine bending mode depends on which of the two N–H bonds is interacting with the B–H bond of the other amine–borane. In other words, it only depends on the relative orientation of the two interacting molecules.

To confirm the existence of DHBs also in solid **1**, we determined the crystal structures of both of its enantiomers from single crystals grown from hexanes.[18] Figure 2 shows a section of the crystal packing for (*R*)-**1** that highlights the DHBs. Unlike in the solid-state structure of the parent $H_3N{\cdot}BH_3$,[4] each $MBA{\cdot}BH_3$ interacts with two adjacent molecules through bifurcated DBHs in a head-to-tail orientation. The two sets of DHBs feature an average bond angle of 147.6° for the N–H···H(B) and 95.8° for the (N)H···H–B bond, respectively (see the Supporting Information, Figure S14 for details). While these angles fit well in the characteristic range, the H–H distances are somewhat long.

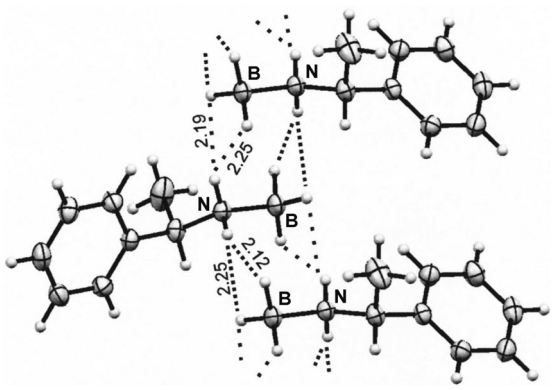

Figure 2. Dihydrogen bonds in the crystal structure of (*R*)-**1**. Distances in Å.

This lengthening might be attributed to steric hindrance introduced by the chiral methylbenzyl substituent. It is interesting to note that the calculated dimer structure which closely resembles the DHB interaction network and relative orientation of the monomers in the crystal structure is not the most stable predicted, but rather the one that is about 0.4 kcal mol^{-1} less favored (for a detailed comparison, see the Supporting Information, Tables S3–S5). On the other hand, the most stable dimer structure identified experimentally in solution is the same as predicted. This suggests that the preferred relative binding arrangement of the two monomeric **1** differs in solid state and in solution.

In summary, the present work is the first study on dihydrogen bonding interactions using VCD spectroscopy. It introduces α-methylbenyl amine–borane **1** as a first interesting representative of a group of chiral amine–boranes, which are ideally suited for the studies. The comparison of experimental and calculated IR and VCD spectra show conclusively that **1** exists as dimer in solution, and the derived structural parameters and interaction energies are comparable to those of the model compound $(H_3N{\cdot}BH_3)_2$. Furthermore, differences in the relative binding arrangements of the two monomeric subunits **1** in solution and in solid state are also revealed. The unique VCD spectral features associated with the dihydrogen bonded dimer may see promising applications in aiding reaction mechanism studies involving DHBs. Rather than relying on solid-state structural determination where differences have been established in this study, such dimeric structures can be probed directly in solution.

Experimental Section

Synthesis of (*R*)-1: The following is for the synthesis of (*R*)-(+)-α-methylbenzylamine–borane adduct (*R*)-**1** and all results were found to be the same for the (*S*)-**1**. A solution of $BH_3{\cdot}DMS$ (1.6 mL, 8.0 mmol, 5.0 M solution in Et_2O) in 20 mL of toluene was prepared and degassed with N_2. To this, an N_2 degassed solution of *(R)*-MBA (1.0 mL, 7.9 mmol) in 20 mL of toluene was added slowly by cannula transfer. The resulting mixture was allowed to stir overnight, during which time a colorless precipitate formed. The supernatant was decanted and the remaining colorless solid was dried in vacuo to afford (*R*)-**1** (816.5 mg, 77 %). $^1H\{^{11}B\}$ NMR (C_6D_6, 500 MHz): $\delta =$ 6.97 (m, 3H, Ar*H*), 6.63 (m, 2H, Ar*H*), 3.59 (m, 1H, C*H*-NH_2-), 3.06

(br, 2H, -NH_2-), 2.21 (s, 3H, -BH_3, assignment made by broadband ^{1}H{^{11}B} decoupling), 1.17 ppm (d, $^3J_{HH}$ = 6.8 Hz, 3H, N-C(H)-CH_3). ^{13}C NMR (C_6D_6, 125 MHz): δ = 142.1 (Ar*C*), 129.0 (Ar*C*), 128.3 (Ar*C*), 126.4 (Ar*C*), 58.2 (N-*C*(H)-CH_3), 19.6 ppm (N-C(H)-*C*H_3). ^{11}B (C_6D_6, 160 MHz): δ = −19.6 ppm (q, $^1J_{BH}$ = 90.7 Hz). HR-MS (EI) *m*/*z*: Calcd. for $[M\text{-}2H]^+$: 133.10628. Found: 133.10610 (Δ = 1.3 ppm).

Computational and further experimental details can be found in the Supporting Information.

Received: March 25, 2014
Revised: May 15, 2014
Published online: July 15, 2014

Keywords: boranes · chirality · dihydrogen bonds · IR spectroscopy · VCD

[1] a) A. Staubitz, A. P. M. Robertson, I. Manners, *Chem. Rev.* **2010**, *110*, 4079 – 4124; b) A. Staubitz, A. P. M. Robertson, M. E. Sloan, I. Manners, *Chem. Rev.* **2010**, *110*, 4023 – 4078.

[2] a) E. Arunan, G. R. Desiraju, R. A. Klein, J. Sadlej, S. Scheiner, I. Alkorta, D. C. Clary, R. H. Crabtree, J. J. Dannenberg, P. Hobza, H. G. Kjaergaard, A. C. Legon, B. Mennucci, D. J. Nesbitt, *Pure Appl. Chem.* **2011**, *83*, 1637 – 1641; b) V. I. Bakhmutov, *Dihydrogen Bonds*: *Principles*, *Experiments*, *and Applications*, Wiley, Hoboken, **2008**.

[3] T. Richardson, S. de Gala, R. H. Crabtree, P. E. M. Siegbahn, *J. Am. Chem. Soc.* **1995**, *117*, 12875 – 12876.

[4] N. J. Hess, G. K. Schenter, M. R. Hartman, L. L. Daemen, T. Proffen, S. M. Kathmann, C. J. Mundy, M. Hartl, D. J. Heldebrant, A. C. Stowe, T. Autrey, *J. Phys. Chem. A* **2009**, *113*, 5723 – 5735.

[5] C. J. Cramer, W. L. Gladfelter, *Inorg. Chem.* **1997**, *36*, 5358 – 5362.

[6] a) M. P. Brown, R. W. Heseltine, *Chem. Commun.* **1968**, 1551 – 1552; b) M. P. Brown, R. W. Heseltine, P. A. Smith, P. J. Walker, *J. Chem. Soc. A* **1970**, 410 – 414; c) M. P. Brown, P. J. Walker, *Spectrochim. Acta Part A* **1974**, *30*, 1125 – 1131.

[7] L. M. Epstein, E. S. Shubina, E. V. Bakhmutova, L. N. Saitkulova, V. I. Bakhmutov, A. L. Chistyakov, I. V. Stankevich, *Inorg. Chem.* **1998**, *37*, 3013 – 3017.

[8] a) J. J. M. Batista, A. N. L. Batista, D. Rinaldo, W. Vilegas, Q. B. Cass, V. S. Bolzani, M. J. Kato, S. N. López, M. Furlan, L. A. Nafie, *Tetrahedron: Asymmetry* **2010**, *21*, 2402 – 2407; b) M. A. Muñoz, O. Muñoz, P. Joseph-Nathan, *Chirality* **2010**, *22*, 234 – 241; c) Y. He, W. Bo, R. K. Dukor, L. A. Nafie, *Appl. Spectrosc.* **2011**, *65*, 699 – 723; d) J. M. Batista, A. N. L. Batista, J. S. Mota, Q. B. Cass, M. J. Kato, V. S. Bolzani, T. B. Freedman, S. N. Lopez, M. Furlan, L. A. Nafie, *J. Org. Chem.* **2011**, *76*, 2603 – 2612; e) K. H. Hopmann, J. Šebestík, J. Novotná, W. Stensen, M. Urbanová, J. Svenson, J. S. Svendsen, P. Bouř, K. Ruud, *J. Org. Chem.* **2012**, *77*, 858 – 869; f) C. Merten, M. Amkreutz, A. Hartwig, *Chirality* **2010**, *22*, 754 – 761.

[9] a) C. Merten, K. Hiller, Y. Xu, *Phys. Chem. Chem. Phys.* **2012**, *14*, 12884 – 12891; b) C. Merten, Y. Xu, *Dalton Trans.* **2013**, *42*, 10572 – 10578; c) A.-C. Chamayou, S. Lüdeke, V. Brecht, T. B. Freedman, L. A. Nafie, C. Janiak, *Inorg. Chem.* **2011**, *50*, 11363 – 11374; d) H. Sato, T. Taniguchi, A. Nakahashi, K. Monde, A. Yamagishi, *Inorg. Chem.* **2007**, *46*, 6755 – 6766; e) H. Sato, Y. Mori, Y. Fukuda, A. Yamagishi, *Inorg. Chem.* **2009**, *48*, 4354 – 4361; f) H. Sato, F. Sato, M. Taniguchi, A. Yamagishi, *Dalton Trans.* **2012**, *41*, 1709 – 1712; g) H. Sato, A. Yamagishi, *Int. J. Mol. Sci.* **2013**, *14*, 964 – 978.

[10] a) K. Monde, N. Miura, M. Hashimoto, T. Taniguchi, T. Inabe, *J. Am. Chem. Soc.* **2006**, *128*, 6000 – 6001; b) H.-Z. Tang, E. R. Garland, B. M. Novak, J. He, P. L. Polavarapu, F. C. Sun, S. S. Sheiko, *Macromolecules* **2007**, *40*, 3575 – 3580; c) T. Kawauchi, J. Kumaki, A. Kitaura, K. Okoshi, H. Kusanagi, K. Kobayashi, T. Sugai, H. Shinohara, E. Yashima, *Angew. Chem.* **2008**, *120*, 525 – 529; d) C. Merten, A. Hartwig, *Macromolecules* **2010**, *43*, 8373 – 8378; e) E. Schwartz, S. R. Domingos, A. Vdovin, M. Koepf, W. J. Buma, J. J. L. M. Cornelissen, A. E. Rowan, R. J. M. Nolte, S. Woutersen, *Macromolecules* **2010**, *43*, 7931 – 7935; f) C. Merten, J. F. Reuther, J. D. DeSousa, B. M. Novak, Phys. Chem. Chem. Phys. **2014**, *16*, 11456 – 11460.

[11] a) M. R. Poopari, Z. Dezhahang, G. Yang, Y. Xu, *ChemPhysChem* **2012**, *13*, 2310 – 2321; b) P. Zhu, G. Yang, M. R. Poopari, Z. Bie, Y. Xu, *ChemPhysChem* **2012**, *13*, 1272 – 1281.

[12] a) C. Merten, M. Amkreutz, A. Hartwig, *Phys. Chem. Chem. Phys.* **2010**, *12*, 11635 – 11641; b) Y. Liu, G. Yang, M. Losada, Y. Xu, *J. Chem. Phys.* **2010**, *132*, 234513.

[13] a) M. Losada, Y. Xu, *Phys. Chem. Chem. Phys.* **2007**, *9*, 3127 – 3135; b) M. Losada, P. Nguyen, Y. Xu, *J. Phys. Chem. A* **2008**, *112*, 5621 – 5627; c) C. Merten, Y. Xu, *Angew. Chem.* **2013**, *125*, 2127 – 2130; *Angew. Chem. Int. Ed.* **2013**, *52*, 2073 – 2076.

[14] a) J. E. Rode, M. H. Jamróz, J. C. Dobrowolski, J. Sadlej, *J. Phys. Chem. A* **2012**, *116*, 7916 – 7926; b) J. E. Rode, J. C. Z. Dobrowolski, *Chirality* **2012**, *24*, 5 – 16.

[15] J.-V. Naubron, L. Giordano, F. Fotiadu, T. Bürgi, N. Vanthuyne, C. Roussel, G. Buono, *J. Org. Chem.* **2006**, *71*, 5586 – 5593.

[16] J. Tomasi, B. Mennucci, R. Cammi, *Chem. Rev.* **2005**, *105*, 2999 – 3094.

[17] a) G. Merino, V. I. Bakhmutov, A. Vela, *J. Phys. Chem. A* **2002**, *106*, 8491 – 8494; b) M. P. Mitoraj, *J. Phys. Chem. A* **2011**, *115*, 14708 – 14716.

[18] CCDC 993481 ((*R*)-**1**) and CCDC 993482 ((*R*)-**1**) contain the supplementary crystallographic data for this paper. These data can be obtained free of charge from The Cambridge Crystallographic Data Centre via www.ccdc.cam.ac.uk/data_request/cif.

